Introduction of Rotors to a Virtual Potentials UUV Trajectory Planning Framework

Matko Barisic*, Zoran Vukic*
Edin Omerdic**

**University of Zagreb, Faculty of Electrical Engineering and Computing,*
Laboratory for Underwater Systems and Technologies, Unska 3, HR-10000 Zagreb, Croatia
(e-mail: {matko.barisic zoran.vukic}@fer.hr)
*** University of Limerick, Limerick, Ireland*
(e-mail: edin.omerdic@ul.ie)

Abstract: A distributed method for online trajectory planning for coordinated UUVs, developed in authors' previous work is revisited. Its design is streamlined with a view towards easy, methodical and robust application in code. A programmatic module for computing command signals necessary and fitting for use with lower-level tracking controllers for te UUV's drives, on the basis of simple numerical formulae for integral and derivative approximations is added. Rotors, a vectorized quantity contributing to local minima avoidance, are introduced. This scheme is compared with the existing strategy for local minima avoidance employed previously within the presented framework. Simulation results are given.

Keywords: Autonomous mobile robots, Gradients, Gradient methods, Trajectory planning, Obstacle avoidance, Co-ordination

1. INTRODUCTION

As shown in authors' previous work (Barisic *et al.* 2006, 2007a, b and c), a framework for online trajectory replanning for UUVs was developed. The framework is suited to coordinated control of UUV schools. Its intent is to provide a foundation for a hierarchical (Barisic *et al.* 2006) distributed control package. The dominant design parameter influencing the structure of the algorithm, as in a large class of similar work by (Beard, R. W. and McLain, T. W. 2003), (Bellingham, J. S. *et al.* 2002) is that it must not rely on communication between UUVs, but rather only sensing. It relies on virtual potentials attributed to obstacles, goal-points of the Itinerary and formations, and thereby is an example of an approach pursued in (Fax, J. A. and Murray, R. M. 2003), (Moreau L. *et al.* 2003) and (Sepulchre R. *et al.* 2005). Similar ground insofar as formations, stability and practical application is concerned, is covered as in (Kalantar, S. and Zimmer, U. 2005) but a different approach is followed. In authors' previous work, a scheme for the avoidance of local minima, consisting of automated insertion/modification of "ghost" goal points was developed (Barisic *et al.* 2007c and d).

Systematized findings of previous research are presented in Section 2. Building blocks of the framework's function-ality are summarized with a clear intent to assure optimal, robust and resilient hard-real time implementation in a future micro-AUV system, based on the commercially available VideoRay Pro ROV, modified into an autonomous system within the authors' principal Laboratory (Stipanov *et al.* 2007). Section 3 concentrates on the introduction of rotors, a scheme of local minima avoidance which is significantly more functionally transparent and modular, scales better and executes faster than "ghost" goal point approach. Section 4 presents evidence to the latter claims by giving simulation results. Section 5 overviews current research towards which the framework described in the paper is aimed, and concludes the paper.

2. THE FRAMEWORK

2.1 Principal features of the framework

The principal framework in this paper is an algorithm for the online replanning of a trajectory which maintains a formation of UUVs in an obstructed theater of operation. The framework has been developed in stages in (Barisic *et al.* 2006, 2007a, b and c; Miskovic *et al.* 2007a and b), wherein details on each aspect of the framework can be found.

The algorithm functions in 2D and is at this stage used for producing the servo command signals for the control of a UUV's trajectory in the surge-sway plane by controlling the course and forward speed. It does so by classifying one of a list of way-points as the current goal-point with a bell-shaped potential distribution function (PDF) in Figure 1. Obstacles detected after passing within the sensor range of an agent ("agent" will be used interchangeably with "UUV") are classified as obstacles of one of: *orthogonal*, *elliptic*, *circular* or *triangular* class. The shape of the orthogonal-class PDF is given for ease of visualization in Figure 2. Other obstacle-classes' PDFs exhibit the same qualitative behavior, but modified by their geometrical properties.

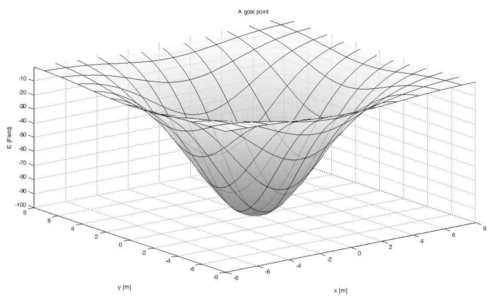

Figure 1: The goal-point PDF

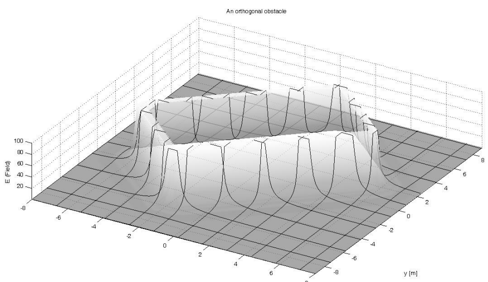

Figure 2: The orthogonal PDF

Mathematical descriptions of the potential distribution functions can be found in Barisic *et al.* 2006, 2007 a, b and c. In a nutshell, the repulsive virtual potential influence of an obstacle E_{obst} is positive and monotonously decreases with r. The latter (r) is a class-defined metric of the point under consideration from the obstacle under consideration. Without going into details of how r is calculated depending on the class of obstacle, the following applies regardless of class:

$$E_{obst}\left(\vec{p}\right) = \exp\left(-A^{+} / r\left(\vec{p}, \vec{p}_{obst}\right)\right) - 1 \tag{1}$$

A^{+} is the repulsion exponent. It is used to regulate the "shyness" of agents i.e. the "severity" with which they regard approaching the obstacle if forced to do so by other potential-generated effects (goal-point behind and near it, being the one agent in a formation that is otherwise, on average, a secure distance from the obstacle wall etc.). r is generally the distance, in the R^2, geometrical sense, between point p and the point on the obstacle's boundary closest to p. It is assumed that the position of the obstacle is defined unanimously and singularly by p_{obst}, a representative point (in vector form) of the obstacle in the same coordinate space as that of p. Accordingly, the calculation of the metric ranges from trivial (circular obstacles) to involved (triangular or elliptic obstacles). The simplest implemented example of such a PDF is the circular obstacle PDF:

$$E_{circ}\left(\vec{p}\right) = \exp\left[-A^{+}_{circ} / \left(\left\|\vec{p} - \vec{p}_{cencirc}\right\| - r_{circ}\right)\right] - 1 \tag{2}$$

Where E_{circ} is the potential at the point p contributed by the circular obstacle, A^{+}_{circ} is the repulsion exponent of the circular obstacle under discourse, $p_{cencirc}$ is the coordinate-vector of the center of the circle and r_{circ} is the radius.

Details for all classes of obstacles included in the framework can be looked up in Barisic *et al.* 2007c and d.

The interaction between coordinating UUVs is realized by having them influence each other as a superposition of repulsive and attractive influences, exemplified by Figure 3. The superposition is between a circular-class obstacle PDF and one or more goal-point PDFs located off-center, depending on the preferred *complete tiling of the plane*. The triangular distribution displayed in Figure 6 will yield a triangular tiling (an infinitely extendible formation wherein the basic cell is an equilateral triangle). More details can be found in Barisic et al. 2007c and d.

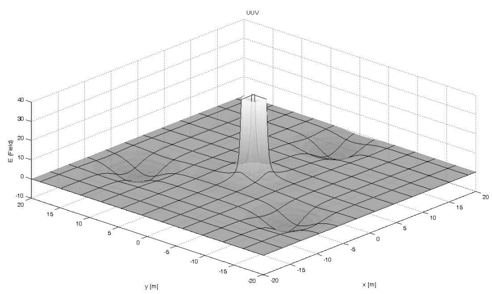

Figure 3: The agent PDF

2.2 Command signals

Isotropic radial sampling of the potential field in the vicinity of the UUV, parameterized by (n_ε, ε), is used to approximate the field's gradient. The approximation includes a quantization error in the vector's argument term, due to quantization steps of $2\pi/n_\varepsilon$, as in Figure 4. Details can be found in Barisic *et al.* 2006, 2007 a, b and c.

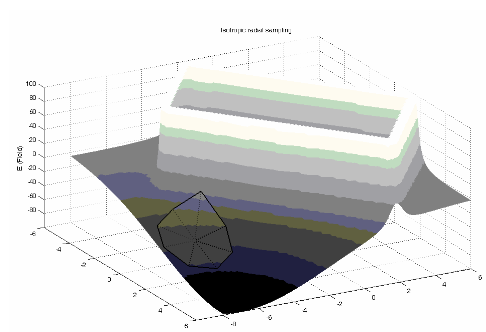

Figure 4: Radial sampling of the potential field

This gradient ∇E, which is a function of k, is taken to be equal to the *propellant force* F by virtue of unit "virtual charge". F is further modified at each time instance by the subtraction of a *virtual friction force* F_{vfric}, dependent on the measured velocity v_m at k–1. This modification ensures the stability of the trajectory-planning algorithm and is developed and described in more detail in Barisic *et al.* 2006, 2007 a, b and c. The norm of F is bounded on the upper side by F_{max} depending on the UUV's operational capabilities (Barisic *et al.* 2006, 2007 a, b, c).

The *reference acceleration vector* $a(k)$ is equated to F by assuming unit “virtual mass” of the agent point.

The acceleration vector is numerically integrated (bilinear formula; Vukic, Z. and Kuljaca, Lj., 2004) to arrive at the *reference velocity vector* $v(k)$. The reference acceleration is also decomposed co-linearly and perpendicularly to $v(k)$:

$$\vec{a}\left(k\right)=\left\langle \vec{a}\left(k\right),\vec{e}_{1}\right\rangle \cdot \vec{e}_{1}+\left\langle \vec{a}\left(k\right),\vec{e}_{2}\right\rangle \cdot \vec{e}_{2} \tag{3}$$

Wherein e_1 and e_2 are an orthonormal base defined by $v(k)$:

$$\left\langle \vec{v}\left(k\right),\vec{e}_{1}\right\rangle = 1 \tag{4}$$

$$\left\langle \vec{v}\left(k\right),\vec{e}_{2}\right\rangle = 0;\ \left\|\vec{e}_{2}\right\| = \left\|\vec{e}_{1}\right\| = 1 \tag{5}$$

The co-linear coefficient is stored as the *surge acceleration command* $a_c(k)$.

$$a_{c}\left(k\right)=\left\langle \vec{a}\left(k\right),\vec{e}_{1}\right\rangle \tag{6}$$

The norm and angle of the reference velocity $v(k)$ are the *surge speed command* – $v_c(k)$ and the *course command* – $\phi_c(k)$, respectively. The speed command is additionally bounded on the upper side by v_{max}, an operational parameter of the UUV (Barisic *et al.* 2007a).

$$v_{c}\left(k\right)=\left\lceil \left\|\vec{v}\left(k\right)\right\|\right\rceil^{v_{max}} \tag{7}$$

$$\phi_{c}\left(k\right)=\arg\left(\vec{v}\left(k\right)\right)=\operatorname{atan2}\left(\vec{v}\left(k\right)\right) \tag{8}$$

The numerical differentiation of the course, $(\phi_c(k)-\phi_c(k-1))/T$ (with T being the sample time) is used to calculate the *rate-of-yaw command* $\omega_c(k)$:

$$\omega_{c}\left(k\right)=\left[\phi_{c}\left(k\right)-\phi_{c}\left(k-1\right)\right]/T \tag{9}$$

The *radius of turn* $r(k)$ is calculated from (6) and (8):

$$r\left(k\right)=\omega_{c}\left(k\right)/v_{c}\left(k\right) \tag{10}$$

This, together with (3), is used to compute the *about-acceleration command*:

$$\alpha_{c}\left(k\right)=\frac{r\left(k\right)\cdot a_{c}\left(k\right)-v_{c}\left(k\right)\cdot\left\{\left[r\left(k\right)-r\left(k-1\right)\right]/T\right\}}{r^{2}\left(k\right)} \tag{11}$$

Equations (6, 7, 9 and 11) provide the derivative and proportional commands for a pair of (supposedly reasonably well) decoupled rate-of-yaw and surge speed controllers at the level “below” the trajectory planner. This “level” stratification is introduced in the sense of a hierarchy described in more detail in Barisic *et al.* 2006.

The integrated difference of the course command $\phi_c(k)$ and the measured course $\phi_m(k)$ can be used to calculate the integral channel dynamics of the rate-of-yaw tracking controller.

The ideal (commanded) position $p_{UUV(c)}$ is calculated by the component-wise bilinear integration of $v(k)$. The norm of the difference between the latter and the measured position, $p_{UUV(m)}$, Δp, is calculated:

$$I_{surge}=\Delta p=\left\|\vec{p}_{UUV(c)}-\vec{p}_{UUV(m)}\right\| \tag{12}$$

This constitutes the integral channel dynamics I_{surge} (possibly modified by a time constant) of the surge speed tracking controller.

The structure and architecture of lower levels of the UUV’s control system undergoing research in the authors’ laboratory is covered in more detail in Stipanov *et al.* 2007 and Miskovic *et al.* 2007a and b.

The system for which the described framework is being specifically developed is a VideoRay Pro II micro-ROV, which has been autonomized by the use of an in-house developed embedded hardware module, mounted externally, dubbed the AutoMarine module. Such a composite craft is referred, in-house as AutoRay. It is a nonholonomic underactuated autonomous mobile robot with 6 degrees of freedom. It is differentially driven in the 2D surge-sway subspace of discourse of this paper. The key performance-degrading issue of this system is strong coupling of pitch to surge action of the thrusters.

However, the herein presented framework is intended to be modular since it assumes the existence of a “lower” level of tracking control which should include both servo-controllers that servo the craft drives according to the signals produced by the presented algorithm, and decoupling controllers which decouple the problematic coupling modes.

3. THE ROTOR POTENTIALS

An approach to local minima avoidance previously included in this framework, and using “ghost” goal-points (GGPs), although effective (Barisic *et al.* 2007 c and d) suffers from a number of drawbacks.

A. Theoretical

A.1. Regardless of the choice of parameters used to define the GGPs, the “detour leg” thus introduced is *in general never (except at random unlikely scenarios) optimal*.

B. Functional (Implementation-related)

B.1. The introduction GGPs burdens the UUV’s onboard memory. This approach requires a second, GGP stack, in addition to the regular Itinerary stack. The size of this stack has a non-deterministic upper bound, heavily dependent upon expected level of clutter in the theater of operation.

B.2. Alternatively, the GGPs can be bundled in with the regular goal points of the Itinerary. However, in addition to being functionally non-transparent, this does not circumvent the memory requirement. Memory is still required to contain an additional address field for keeping the GGPs within proper context within the amalgamated Itinerary. This address field has a non-deterministic upper bound.

B.3. The introduction of either of these two approaches also, due to processing overhead, thus encumbering the CPU in addition to the memory. Consequently, the hard-real-time performance is compromised.

In order to approach the local minima avoidance problem from a different perspective, a rotor component is added to the stator PDF description of obstacles.

The rotor introduces a rotary "sliding slope" of potential, "shoving" the agent around an obstacle by virtue of the slope rotating about the barycenter of the obstacle, as exemplified by Figure 5.

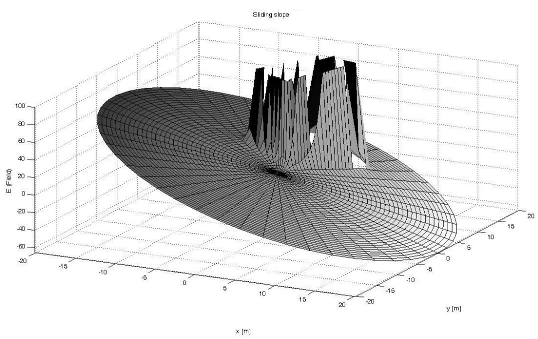

Figure 5: "Sliding slope" effect of a rotor

The stator part of every obstacle class's PDF is given irrespective of geometry, dependent solely on the metric. In marked contrast, the rotor PDF is a vector. Therefore, it possesses a direction, which relies on the agent-relative geometry of the theater of operations (more specifically, the obstacle in question in relation to the goal-point). The dependence of the direction θ of the rotor vector on the geometry is given by equations (13 – 16) which geometric interpretation is presented in Figure 6.

$$\gamma_{obst}^{GP} = \arg\left(\vec{p}_{obst} - \vec{p}_{GP}\right) = \mathrm{atan2}\left(\vec{p}_{obst} - \vec{p}_{GP}\right) \tag{13}$$

$$\gamma_{UUV}^{GP} = \arg\left(\vec{p}_{UUV} - \vec{p}_{GP}\right) = \mathrm{atan2}\left(\vec{p}_{UUV} - \vec{p}_{GP}\right) \tag{14}$$

$$d = \begin{cases} 0.5\,\mathrm{sgn}\left(\gamma_{obst}^{GP} - \gamma_{UUV}^{GP}\right) - 0.5; & \mathrm{sgn}\left(\gamma_{obst}^{GP} - \gamma_{UUV}^{GP}\right) \neq 0 \\ -1 & \gamma_{obst}^{GP} = \gamma_{UUV}^{GP} \end{cases} \tag{15}$$

$$\theta = \mathbf{R}\left(d\pi / 2\right) \cdot \delta_{UUV}^{obst} \tag{16}$$

In these equations, R(.) is the rotation matrix, d is the rotor direction (1 is clockwise and –1 is anticlockwise) and γ is the symbol used for the relative azimuth (bearing). Superscript indices mark the point of reference and the subscript ones the point whose azimuth is calculated. Indices have the following meanings: *obst* – obstacle (barycenter); *GP* – goal point (a singular point); *UUV* – the UUV under consideration.

δ_{UUV}^{obst} is the normal angle, directed from the UUV towards the obstacle. However, it is *not generally* the azimuth of the obstacle's barycenter relative to the UUV (except in the trivial case of a circular obstacle). Rather, it is the inwards normal to the point of the obstacle's boundary closest to the UUV, as displayed in Figure 9.

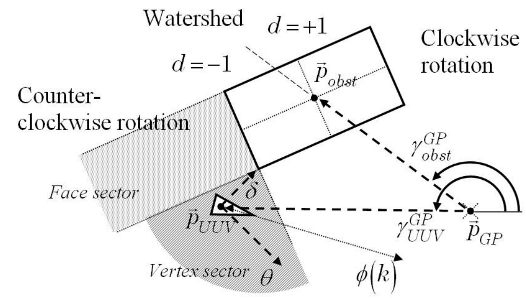

Figure 6: Relationships between the agent-relative geometry and θ

In addition to coding equations (13 – 16) into the framework, a cut-off metric beyond which the rotor part of the potential influence is disregarded was included for functional reasons. This produces the representation of the rotor part of the potential influence of an obstacle, displayed in Figure 7 (orthogonal class is used for clarity).

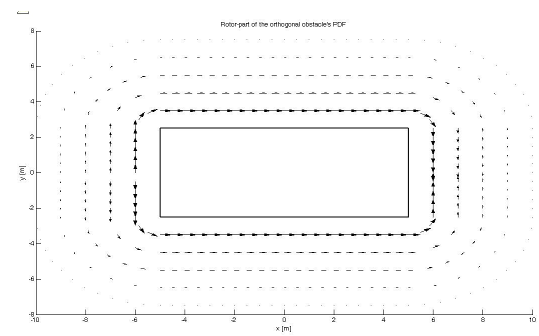

Figure 7: The rotor part of an orthogonal obstacle class PDF

4. SIMULATION

In this paper, simulation was confined to measuring the effects of the new rotor based approach against an already developed local minima avoidance scheme based on "ghost" goal points. The discussion of the necessity of including some scheme of local minima avoidance, an example local minimum lock, and the resolution of the lock by virtue of this previously developed scheme is detailed in (Barisic *et al.* 2007b and c). A simulation of online trajectory planning was run in order to compare the rotor and "ghost goal point" approaches for an unrealistically cluttered theater of operation within which a single UUV (for clarity of graphical results) is navigating. Figure 8 displays the trajectory obtained by the use of rotor-inclusive PDFs of obstacles. Figure 9 displays the earlier, "ghost goal point" method trajectory. Figure 10 gives the comparison of speed commands.

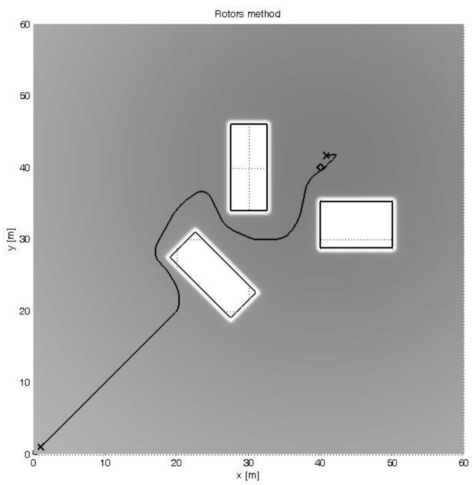

Figure 8: Trajectories planned by rotor-inclusive obstacle PDFs (ROT method)

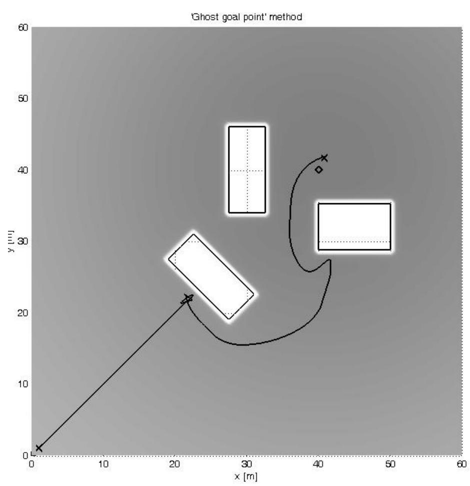

Figure 9: Trajectories planned by the ghost goal point method (GGP method)

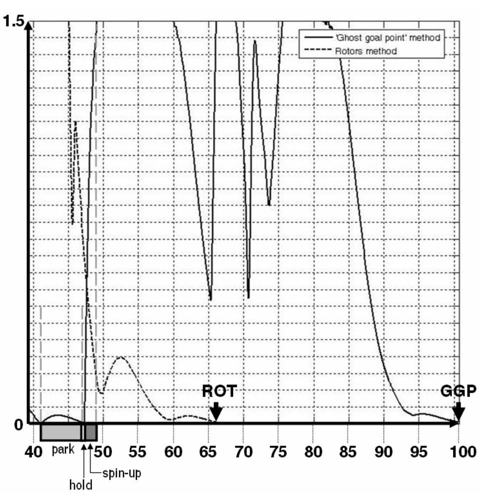

Figure 10: Comparison of surge speed command signals after 40s of simulation

As is visible from the preceding figures, the "ghost goal point" method produces a suboptimal trajectory, both in terms of the length of path, and the time of termination. The difference between the time it takes to execute both variants is 400 sampling intervals of 0.1s each, in favor of the rotor-method. For a fair comparison, certain parts of the GGP method which can be further optimized need to be discarded from the comparison. Parking at the ghost goal point is defined as the 1s interval during which the UUV is nearly stationary, before the logic activates the "deletion" of a ghost goal point from the temporary Itinerary and reintroduces the original one. After the original goal point is reintroduced (and prior to "parking"), 3 – 5s are expended in "parking approach" or "spinning up to top cruise speed", respectively. Added together, (taking the upper bounds of 5s on the "parking approach" and "spin-up") this amounts to 11s of time taken out of consideration per ghost goal point necessary in navigation. Since in the example, there were 2 such occurrences in Figure 9, the time of completion can be regarded as being 101–22 = 79s. When compared to 66s of rotor-method trajectory, the GGP method is therefore 19.7% slower at the final goal point, or conversely, the ROT method is 16.5% faster. Also, the shape of the planned trajectory of the ROT method will always be more spatially compact, since with the GGP method the compactness depends on the values of independent parameters used to perform the calculation of the ghost goal point's position (cf. Barisic *et al.* 2007b and c). Furthermore, the ROT method velocity command displays far less variation, translating into less jerky action of the thrusters and far less (square law) energy consumption, which is a penultimate consideration in autonomous systems.

5. CONCLUSION

5.1 Overview

In conclusion, a framework for effective, fast and robust on-line trajectory replanning is presented. A functionally transparent and modular approach of including rotor components into obstacle models is demonstrated and tested in simulation against an existing local minima-avoidance scheme. It is demonstrably superior to the previously adopted scheme in terms of performance and implementation-related issues.

The proposed framework is intended to be used as a "middle" level of a hierarchical (cf. Barisic *et al.* 2006) intelligent control system for coordinated UUVs under development in the authors' laboratory.

The hierarchical tier of the presented framework above the level of the immediate UUV drive control is self-evident from the fact that the framework delivers on-line command signals for such servo- and decoupling-controllers. By having the trajectory planning performed by the framework, the problem of using various controller design techniques is efficiently *separated* from the trajectory planning problem.

The hierarchical tier of the framework below the level of high-intelligence software engines like mission control languages, fault accommodation frameworks etc. is also evident. The proposed framework, namely, *abstracts* the guidance problem sufficiently that it can be incorporated into semantic programming.

5.2 Future research

Future research will be directed in three directions:

A. Eliminating "parking creep" and "smoothing" the dynamics of formations

B. Including a diffeomorphism alike to the one proposed by Fadenza P. V. and P. U. Lima (2007) which will alleviate the problem of controller design, thereby allowing synthesis of a larger class of optimal control laws.

C. Observing/estimating the trends and attributes of error-signals of the lower level feedback loops. These can be used to model stationary disturbances or faulty conditions.

ACKNOWLEDGMENTS

This research is supported by The "*RoboMarSec - Underwater robotics in sub-sea protection and maritime security*" project, no. 036-0362975-2999, of the Ministry of Science, Education and Sports of the Republic of Croatia.

This research is also supported by financial and infrastructural resources of the "*Center for Underwater Systems and Technologies*" (*CUST*), a Croatian-based non-for-profit organization of maritime engineering and research professionals.

REFERENCES

Barisic, M., Z. Vukic and N. Miskovic (2006). Design of a coordinated control system for marine vehicles. In: *Proceedings of the 6th IFAC Conference on Manoeuvring and Control of Marine Craft* (Pascoal, A.), on CD. Instituto Superior Technico, Lisabon, Portugal.

Barisic, M., Z. Vukic and N. Miskovic (2007). Kinematic Simulative Analysis of Virtual Potential Field Method for AUV Trajectory Planning. In: *Proceedings of the 15th Mediterranean Conference on Control and Automation*, (Valavanis K. and Kovacic, Z.), on CD. Mediterranean Control Association, Athens, Greece.

Barisic, M., Z. Vukic and N. Miskovic (2007). A Kinematic Virtual Potentials Trajectory Planner For AUV-s. In: *Proceedings of the 6th IFAC Symposium on Intelligent and Autonomous Vehicles*, (Devy, M.), on CD. Laboratoire d'Architecture et d'Analyse des Systèmes, Toulouse, France.

Barisic, M., Z. Vukic, N. Miskovic and B. Tovornik (2007). AUV Formations Achieved By Virtual Potentials Trajectory Planning In A Simulated Environment. In: *Proceedings of the 7th IFAC Conference on Control Applications in Marine Systems*, (Vukic, Z. and Longhi, S.), on CD. Center for Underwater Systems and Technologies, Zagreb, Croatia.

Beard, R. W. and McLain, T. W. (2003). Multiple UAV Cooperative Search under Collision Avoidance and Limited Range Communication Constraints. In: *Proceedings of the 42nd IEEE Conference on Decision and Control*, pp. 25-30

Bellingham, J. S. et al. (2002). Cooperative Path Planning for Multiple UAVs in Dynamic and Uncertain Environments. In: *Proceedings of the 41st IEEE Conference on Decision and Control,* pp. 2816-2822

Fadenza, P. V. and P. U. Lima (2007), Non-holonomic robot formation with obstacle compliant geometry. In: *Proceedings of the 6th IFAC Symposium on Intelligent and Autonomous Vehicles*, (Devy, M.), on CD. Laboratoire d'Architecture et d'Analyse des Systèmes, Toulouse, France.

Fax, J. A. and Murray, R. M. (2004). Information Flow and Cooperative Control of Vehicle Formations. In: *IEEE Transactions on Automatic Control,* vol. 49, issue 9, pp. 1465-1476

Kalantar, S. and Zimmer, U. (2005). Motion planning for small formations of autonomous vehicles navigating on gradient fields. In: Proceedings of *The International Symposium on Underwater Technology, UT 2007 - International Workshop on Scientific Use of Submarine Cables and Related Technologies 2007* (Ura, T., Wernli R. and Kasahara J.), pp 512-519. Institute of Industrial Science, University of Tokyo, Tokyo, Japan.

Miskovic, N., Z. Vukic, and M. Barisic (2007). Transfer Function Identification by Using Self-Oscillations. In: *Proceedings of the 15th Mediterranean Conference on Control and Automation*, (Valavanis K. and Kovacic, Z.), on CD. Mediterranean Control Association, Athens, Greece.

Miskovic, N., Z. Vukic, M. Barisic and P. P. Soucacos (2007). AUV Identification by Use of Self-Oscillations. In: *Proceedings of the 7th IFAC Conference on Control Applications in Marine Systems*, (Vukic, Z. and Longhi, S.), on CD. Center for Underwater Systems and Technologies, Zagreb, Croatia.

Moreau, L., Bachmeyer, R. and Leonard, N. E. (2003). Coordinated Gradient Descent: A Case Study of Langrangian Dynamics With Projected Gradient Information. In: *Proceedings of the 2nd IFAC Workshop on Lagrangian and Hamiltonian Methods for Nonlinear Control*, Universidad de Sevilla, Sevilla, Spain.

Sepulchre, R., Paley, D. and Leonard, N. E. (2005). Graph Laplacian and Lyapunov Design of Collective Planar Motions. In: *Proceedings of the International Symposium on Nonlinear Theory and Its Application* (Oishi, S. and Vandewalle, J.), The Institute of Electronics, Information and Communication Engineers, Tokyo, Japan.

Stipanov, M., N. Miskovic, Z. Vukic and M. Barisic (2007). ROV Autonomization - Yaw Identification and Automarine Module Architecture. In: *Proceedings of the 7th IFAC Conference on Control Applications in Marine Systems*, (Vukic, Z. and Longhi, S.), on CD. Center for Underwater Systems and Technologies, Zagreb, Croatia.

Vukic, Z. and Lj. Kuljaca (2004). *Automatic Control: Analysis of linear systems*, Kigen, Zagreb, Croatia.